

ASIAN JOURNAL OF PHYSICS

An International Peer Reviewed Research Journal

Advisory Editors : W. Kiefer, FTS Yu, Maria J Yzuel

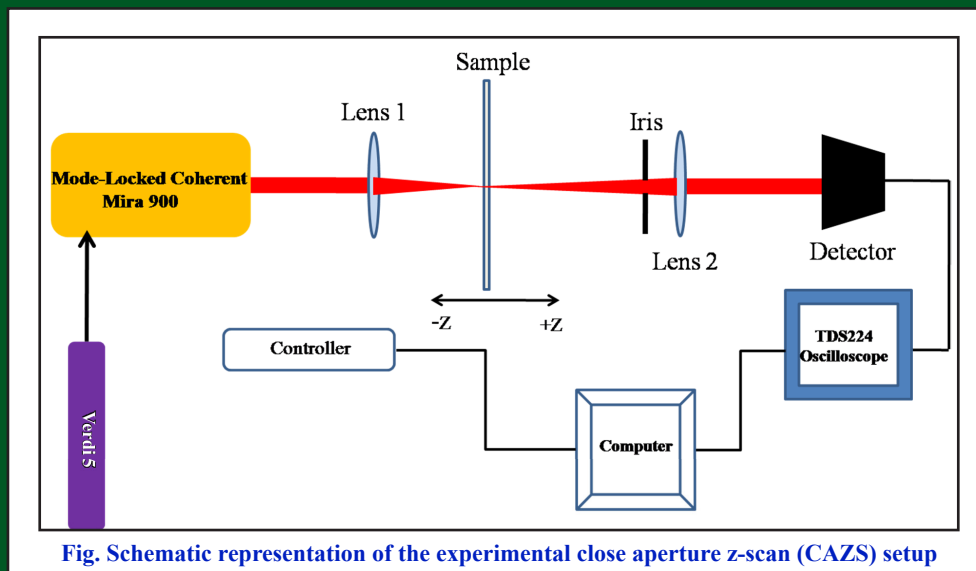


Fig. Schematic representation of the experimental close aperture z-scan (CAZS) setup

Guest Editors : D Goswami, R Kulkarni & G Rajshekhar



ANITA PUBLICATIONS

FF-43, 1st Floor, Mangal Bazar, Laxmi Nagar, Delhi-110 092, India
B O : 2, Pasha Court, Williamsville, New York-14221-1776, USA



Analytical model of band rejection filter based on multimode-single mode-multimode fiber concatenation structure

Protik Roy and Partha Roy Chaudhuri

Department of Physics, Indian Institute of Technology, Kharagpur -721 302, India, India

Here, we propose a novel all-fiber band rejection filter utilizing multimode-single mode-multimode (M-S-M) concatenated structure. The proposed filter consists of two identical multimode fibers (MMFs) and a conventional single-mode fiber (SMF) of a very small length, which is spliced between the MMFs. Since there is a core diameter difference between MMF and SMF, the cladding of the SMF are excited along with core modes and an interference loss between core mode and cladding modes is observed. By systematically adjusting the parameters of fibers of the proposed device, we show that the interference loss in the device can be utilized as a band rejection filter. © Anita Publications. All rights reserved.

Keywords: Optical fiber filter, Modal overlap, Core and cladding modes, Modal interference.

1 Introduction

Wavelength band rejection filters are useful and basic devices in various areas of fiber circuits, photonic research and instrumentation. A key use of these filters is in telecommunication systems, where a particular band of wavelengths is required to be discarded in the optical signal. This type of filter has a large number of applications in different fields ranging from temperature, curvature sensors [1,2] to band rejection filters and attenuators for fiber lasers [3,4]. Wavelength band rejection filters are also used in directional couplers [5] as well as Erbium-doped fiber amplifiers (EDFAs) gain equalization [6]. The significant key aspect of band rejection filter to be considered is its ability to tune any desired wavelength band. In earlier reported works, band rejection filters were mainly based on long period grating(LPG)[7-9] and straight fiber Bragg grating (FBG) [10,11]. One of the significant constraints of these band-rejection filters is the difficulty to obtain a dynamic wavelength trimming over a desirable band spectrum. Although many other reported methods were specially focused on electrical [12], thermo-optical [13-15], and magnetic [16] tuning using photonic crystal fibers or FBGs, but tuning of desired wavelength band was still limited. With this intention in mind, in this work, we report a dynamic band trimming method by using an in-line M-S-M fibers concatenation structure. Then by realizing the CDM between MMFs and SMF, we design and demonstrate an M-S-M model. The proposed model depends on the interference loss resulting from the mode coupling of the cladding modes with the guided modes at the splicing junction. By systematically adjusting the parameters of the fibers in the M-S-M structure, the transmission loss in the interference spectrum can be utilized as a band rejecting filter. Using our analytical model, we study the representative cases as investigated and reported in Refs [17,18] and compare our analytical results with those obtained experimentally. Thus, we validate our description of mode-coupling model. In the following, we present the method of analysis of the proposed device and demonstrate some key results.

Corresponding author

e mail: roycp@phy.iitkgp.ac.in (Partha Roy Chaudhuri)

2 Filter structure and operating mechanism

Figure 1 shows the schematic of the proposed band rejection filter. The design incorporates a short SMF segment of length L , which is sandwiched between two conventional step-index MMFs. Due to the core diameter difference at MMFs and SMF splicing junction, when the light passes through the first MMF and falls into the central SMF, the guided modes of the first MMF couple to the core mode and as well as the cladding modes of the central SMF. Thus, the several cladding modes of the central SMF are excited alongwith the fundametal mode of the same SMF. Any change within the medium of certain refractive index surrounding the central SMF cladding region modulates the way light is transmitted along the fiber. We, outline our model of light propagation through this structure that illustrates the principle of band rejection filter and enables us to interpret experimental results [1] analytically in the following.

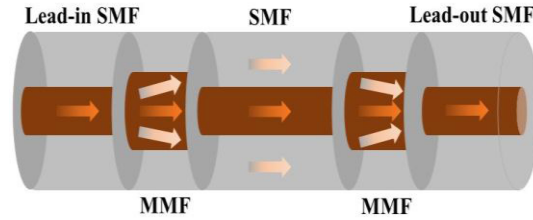


Fig 1. Schematic of the proposed filter.

When the light passes through the lead-in SMF falls on the first MMF segment, it excites not only the fundamental core mode but also several higher order modes. At the lead-in SMF- 1st MMF interface, we can express the total field as

$$E(r, 0) = \sum_{q=1}^m b_q M_q \quad (1)$$

where $E(r, 0)$ represents the fundamental mode of the lead-in SMF. Each of the mode of first MMF and the total number of modes that MMF can accommodate are denoted as M_q , and m , respectively. The excitation coefficients of each mode, expressed as b_q in the first MMF section, can be estimated as,

$$b_q = \frac{\int_0^\infty E(r, 0) M_q r dr}{\int_0^\infty M_q M_q r dr} \quad (2)$$

After covering the first MMF of length L_1 , the field distribution becomes,

$$E(r, L_1) = \sum_{q=1}^m b_q M_q e^{i\beta_q L_1} \quad (3)$$

where the propagation constant of the q th order mode is denoted as β_q . Because of the mismatch between core diameters of MMF and SMF, the modes of MMF couple with the fundamental core mode and the major cladding modes of the central SMF for the light transmission from the 1st MMF to the central SMF. Out of all, only azimuthally symmetric modes (LP_{lm} , where $l = 0$ and $m = 0, 1, 2, \dots$) can survive this light transmission [48]. So, throughout the analysis, we only take azimuthally symmetric modes. Even though, the MMF can accommodate hundreds of modes (LP_{0m}), the effect of the higher order modes pf MMF is negligible and constrained to this mode coupling owing to the core- diameter difference between the MMF and the SMF [19]. Simulating the contribution of the two modes (LP_{01} and LP_{02}), it is found that these two contribute significantly to the mode coupling and hence, in our analytical analysis, we only consider LP_{01} and LP_{02} and neglect any contribution of the higher order modes. If $S_p(r, 0)$ be the p th mode of the central SMF ($p = 1$ for core mode and $p > 1$ for cladding modes), then after traversing the first MMF light becomes,

$$E(r, L_1) = \sum_{p=1}^n c_p S_p \quad (4)$$

where c_p , the excitation coefficient of each mode, can be calculated as,

$$c_p = \frac{\int_0^\infty E(r, L_1) S_p r dr}{\int_0^\infty S_p S_p r dr} \quad (5)$$

In general, after traversing through the central SMF, the amplitude of the p^{th} core/cladding mode can be expressed as,

$$E_p(r, L) = c_p S_p e^{i\beta_p L} \quad (6)$$

where β_p is the p^{th} core/cladding mode propagation constant. Again, for light transmission from SMF to the last MMF, the higher order cladding modes of the central SMF contribute negligibly to the mode coupling. Hence, in our approach, only $p = 2$ is considered. Therefore, for this light propagation, we consider the mode coupling of the SMF core mode to the LP₀₁ and LP₀₂ modes of the second MMF, and the coupling of the cladding mode corresponding to $p = 2$ to the two last MMF modes of the lowest orders.

Now, the intensity of the p^{th} mode after travelling the central SMF, can be written as,

$$I_p = |E_p^*(r, L) \cdot E_p(r, L)| \quad (7)$$

After traversing through the central SMF, these cladding modes and only core mode of central SMF interfere with each other and recombine in the last MMF segment; and the corresponding interference intensity is estimated as

$$I = I_1 + I_p + 2\sqrt{I_1 I_p} \cos(2\pi \Delta n_{eff}^p L/\lambda) \quad (8)$$

$$\Delta n_{eff}^p = n_{core} - n_{clad}^p \quad (9)$$

In Eq (8), the intensities of the core mode and the p th order cladding mode are expressed as I_1 and I_p , respectively. The effective refractive indices of the core mode and the p th cladding mode are expressed as n_{core} and n_{clad}^p , respectively. As explained earlier, here, only the main interference between the cladding mode corresponding to $p = 2$ and the core mode is considered in the analysis. For destructive interference, the difference in the phases between the core mode and the p th order cladding mode generally satisfies,

$$\frac{2\pi \Delta n_{eff}^p L}{\lambda_{dip}} = (2t + 1)\pi, \quad t = 0, 1, 2, \dots \quad (10)$$

Thus, λ_{dip} can be calculated as

$$\lambda_{dip} = \frac{2\Delta n_{eff}^p L}{(2m + 1)} \quad (11)$$

Total transmission (T) of the proposed M-S-M structure will be,

$$T = \frac{\int_0^\infty I r dr}{\int_0^\infty |E(r, 0)|^2 r dr} \quad (12)$$

In the output spectrum of the proposed device, the interference loss, I (Eq 8), between the guided mode and cladding modes of the central SMF can be adjusted by varying the parameters of the fibers to reject any desirable wavelength band.

3 Results and Discussion

To verify our analytical approach, we have computed the transmittance spectrum of the filter device (Fig 3). The corresponding parameters are given in Table 1. The choice of these parameters owe to the fiber used in the experimental investigation reported in [17]. We compared our computed result with that reported experimentally [17]. Although, our computed transmittance exhibits more interference loss due to the chosen

parameters, our result predicts the nature of variation in transmittance recorded experimentally [17] very well. The full width at half minimum is reported to be 35 nm in the experiment while our result shows a bandwidth of 40 nm at full width at half minimum.

Table 1. Parameters used in the simulation for an external medium (Refractive Index 1.42)

Fiber type (length)	Core/Clad RI	Core/Clad diameter (μm)	V number
SMF (3 mm)	1.4608-1.4577/1.4594-1.4563	6.2/60	2.3498-2.0395
MMF (2 mm)	1.4708-1.4677/1.4508-1.4477	24/60	34.3883-29.8468

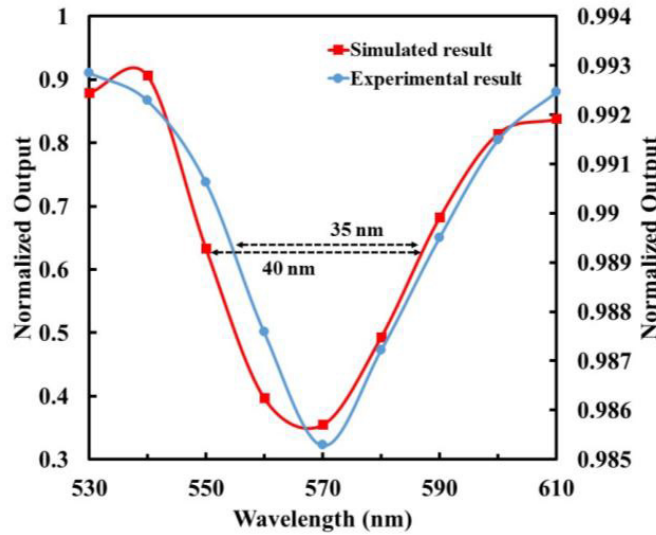


Fig 2. Experimental [17] and simulated result of transmission spectrum

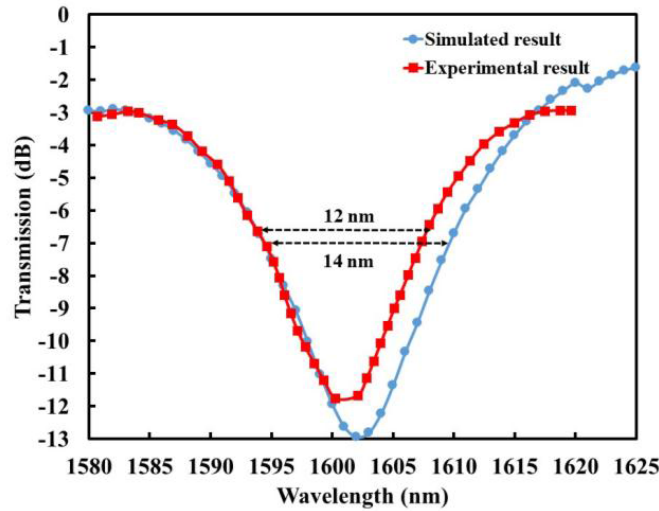


Fig 3. Experimental [18] and simulated result of transmission spectrum.

In Fig 3, we show a comparison between our simulated result and experimentally observed result [18]. Evidently, our result fairly predicts the experimentally obtained characteristics. Table 2 shows the parameters

of the proposed device considered during the simulation. In the experiment, the full width at half minimum is reported to be 12 nm while our result shows a bandwidth of 14 nm at full width at half minimum. It is easy to observe that by systematically changing the fibers' parameters of the device, our M-S-M configuration shows a similar variation as that of obtained experimentally. Our proposed model involves a simple structure and a general formulation which makes this device unique from the other available devices.

Table 2. Parameters used in the simulation for an external medium (Refractive Index 1.42)

Fiber type (length)	Core/Clad RI	Core/Clad diameter (μm)	V number
SMF (5 mm)	1.4437-1.4431/1.4337-1.4331	7/60	2.3609-2.2951
MMF (2 mm)	1.5037-1.5031/1.4937-1.4931	30/60	10.3272-10.0393

4 Conclusion

We report here a new approach to design and tune an only-fiber band rejection filter depending on interference loss of co-propagating cladding and core modes in a fiber structure. The device comprises of a short SMF section, spliced between two identical MMFs. Due to the core diameter difference between MMF and SMF, cladding modes of the central SMF get excited and interfere with the core mode of the central SMF when they recombine at the last MMF. This destructive interference loss in the interference spectrum of the output can be utilized to reject any desirable wavelength band. Using this analysis and by changing the parameters of the device, we predict the normalized output at different source wavelengths. These analytically computed results match very well with those recorded from the experiments [17 and 18]. Our analytical approach is general and can be readily implemented to configure such MMF-SMF-MMF concatenated structure or any higher order concatenated cladding mode based devices.

Acknowledgements

Authors acknowledge the financial support of the Institute grant of IIT Kharagpur, India to carry out the research described in this article.

References

1. Rugeland P, Margulis W, Revisiting twin-core fiber sensors for high-temperature measurements, *Appl Opt*, 51(2012) 6227–6232.
2. Guzman-Sepulveda J R, Dominguez-Cruz R, Sanchez-Mondragon J J, May-Arrijoja D A, Curvature sensor based on a two-core optical fiber, *Proc Conf Lasers Electro-Opt*, 1(2012)JW2A-116.
3. Vengsarkar A M, Lemaire P J, Judkins J B, Bhatia V, Erdogan T, Sipe J E, Long-period fiber gratings as band-rejection filters, *J Light Technol*, 14(1996)58–65.
4. Yun S H, Hwang I K, Kim B Y, All-fiber tunable filter and laser based on two-mode fiber, *Opt Lett*, 21(1996)27–29.
5. Vallée R, Drolet D, Practical coupling device based on a two-core optical fiber, *Appl Opt*, 33(1994)5602–5610.
6. Marques C A F, Oliveira R A, Pohl A A P, Nogueira R N, Adjustable EDFA gain equalization filter for DWDM channels based on a single LPG excited by flexural acoustic waves, *Opt Commun*, 285(2012)3770–3774.
7. Lin C Y, Wang L A, A wavelength- and loss-tunable band-rejection filter based on corrugated long period fiber grating, *IEEE Photon Technol Lett*, 13(2001)332–334.
8. Kim J, Paek U C, Lee B H, Hu J, Marks B, Menyuk C R, Impact of interstitial air holes on a wide bandwidth rejection filter made from a photonic crystal fiber, *Opt Lett*, 31(2006)1196–1198.
9. Chavez R I M, Rios A M, Gomez I T, Chavez J A A, Aguilar R S, Ayala J E, Wavelength band rejection filters based on optical fiber fattening by fusion splicing, *Opt Laser Technol*, 40(2008)671–675.
10. Canning J, Psaila D C, Brodzeli Z, Higley A, Janos M, Characterization of apodized fiber Bragg gratings for rejection filter applications, *Appl Opt*, 36(1997)9378–9382.

11. Chen D R, Yang T J, Wu J J, Shen L F, Liao K L, He S L, Band-rejection fiber filter and fiber sensor based on a Bragg fiber of transversal resonant structure, *Opt Express*, 16(2008)16489–16495.
12. Du F, Lu Y Q, Wu S T, Electrically tunable liquid-crystal photonic crystal fiber, *Appl Phys Lett*, 85(2004)2181–2183.
13. Bae J K, Kim S H, Kim J H, Bae J, Lee S B, Jeong J M, Spectral shape tunable band-rejection filter using a long-period fiber grating with divided coil heaters, *IEEE Photon Technol Lett*, 15(2003)407–409.
14. Sohn K R, Kim K T, Thermo-optically tunable band-rejection filters using mechanically formed longperiod fiber gratings, *Opt Lett*, 30(2005)2688–2690.
15. Zhao Z Y, Tang M, Liao H Q, Ren G B, Fu S N, Yang F, Shum P P, Liu D M, Programmable multi-wavelength filter with Mach-Zehnder interferometer embedded in ethanol filled photonic crystal fiber, *Opt Lett*, 39(2014)2194–2197.
16. Zu P, Chan C C, Gong T X, Jin Y X, Wong W C, Dong X Y, Magneto-optical fiber sensor based on bandgap effect of photonic crystal fiber infiltrated with magnetic fluid, *Appl Phys Lett*, 101(2012)241118; doi. org/10.1063/1.4772017.
17. Biswas R, Karmakar P, Gogoi C, Sarma D, A comparative analysis of hetero core spliced msm and sms system in terms of transmittance, *Int J Opt Photonics*, 3(2017)16–19.
18. Javorsky B, Silva R E, Pohl A A P, Wavelength tunable filter based on acousto-optic modulation of a double-core fiber, *IEEE Photon Technol Lett*, 31(2019)1135–1138.
19. Roy P, Chaudhuri P R, Characteristics of cladding mode-based refractive index sensor using MMF-SMF-MMF configuration, *J Opt*, 2022.

[Received: 22.09.2022; revised recd: 26.10.2022; accepted: 30.10.2022]



Protik Roy received his M Sc degree from the Indian Institute of Technology, Kanpur, India in 2018. In 2019, he joined the Physics Department, Indian Institute of Technology, Kharagpur, West Bengal, India, as a Research Scholar. Since then, he has been working under the supervision of Prof Partha Roy Chaudhuri for his Ph D degree. His main research interest is Fiber optic sensors based on Cladding mode.



Partha Roy Chaudhuri is Professor of Physics at Indian Institute of Technology Kharagpur, working in the area of Fiber and Integrated Optics and Photonics. In 2000, he did his Ph D from the Fiber Optics Group of Indian Institute of Technology Delhi. He then pursued postdoctoral research in the Kyoto Institute of Technology, Japan, as a Japanese Government Fellow where he was working on various optical waveguides and components. Later, during 2002-2004, he worked in the Institute for Communications Research, NUS, in experimental research with photonic crystal fibers and components. In 2004, he joined the Faculty of the Physics Department, IIT Kharagpur. He has successfully carried out (and is working as PI and Co-PI on) several Sponsored Research projects funded by Government Agencies namely, DST, DRDO, BRNS, MHRD with industry (IMPRINT) that led to deliverables, development of Technical Know-hows, Copyrights and Patent filing. He is involved with collaboration research with institutes in India and abroad. Over this period he has supervised/is supervising twelve Ph D theses, postdocs and more than thirty five M.Tech and MSc. Project theses. He published more than 95 research papers and contributed invited chapters in six books. His NPTEL course on Modern Optics has received wide appreciation of researchers from India and abroad. He is a member of Opt Soc of America (OSA), Opt Soc of India (OSI), KIT Educational Exchange Club, Inst of Electron and Tel Engg. (IETE), Indian National Science Association. His current research interests are in the area of microstructured optical fibers/photonic crystal waveguides and devices for passive and active/nonlinear applications and development of fiber optic sensors for detection of weak electric and magnetic fields.

Dr Partha is Editor of Asian J Phys.